Atomic Ensemble and Electronic Effects in Ag-Rich AgPd Nanoalloy Catalysts for Oxygen Reduction in Alkaline Media

Daniel A. Slanac[a], William G. Hardin[d], Keith P. Johnston[a,c,d]*, and Keith J. Stevenson[b,c,d]*

[a]Department of Chemical Engineering (1 University Station C0400), [b]Department of Chemistry and Biochemistry (1 University Station A5300), [c]Center for Electrochemistry, and [d]The Texas Materials Institute, The University of Texas at Austin, Austin, TX 78712

*Keith J. Stevenson: stevenson@cm.utexas.edu
*Keith P. Johnston: kpj@che.utexas.edu

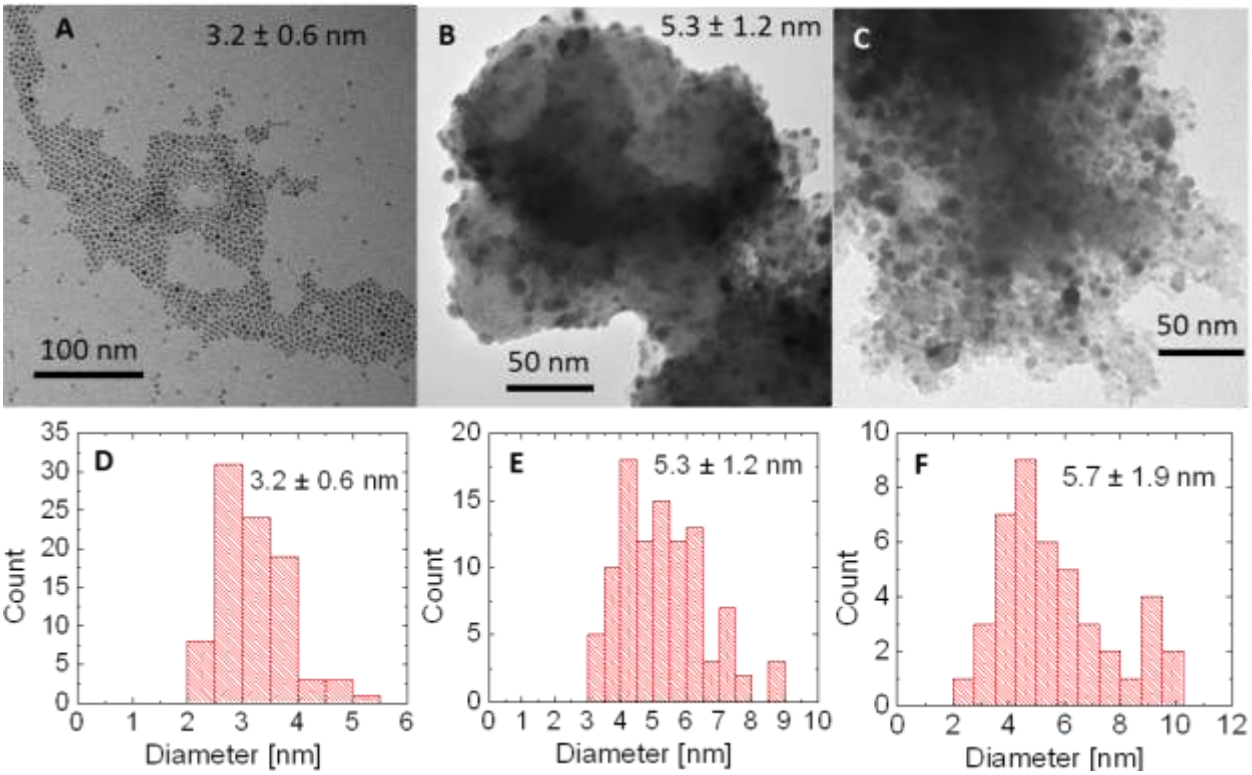

Figure S1: Low mag TEM micrographs of (A) as-synthesized Ag_9Pd nanoparticles, (B) Vulcan XC72 carbon supported Ag_9Pd particles after calcination at 450°C in N_2, and (C) commercial Pd/VC calcined at 450°C N_2. The alloy particles undergo slight sintering from 3.2 to 5.3 nm. The similar size of the alloy and the commercial catalyst after calcination allows for meaningful comparison of activities based on their similar surface/volume ratio.

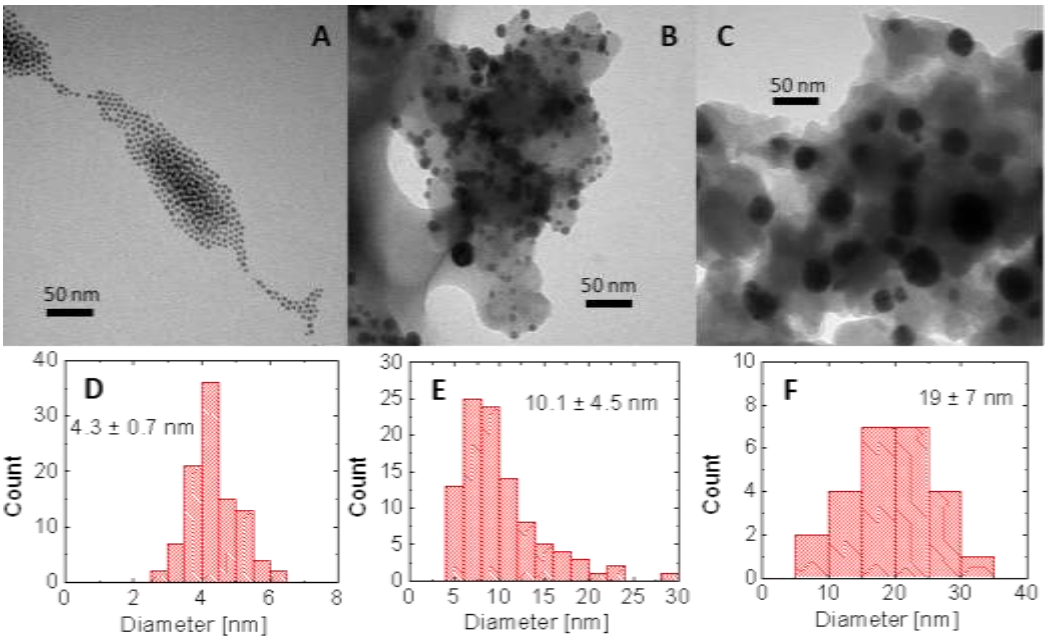

Figure S2: TEM for pure Ag nanoparticles (A) as-synthesized and after adsorption on Vulcan XC72 carbon and calcination at (B) 210°C in H_2/N_2 and (C) 450°C in N_2. The particles sinter significantly for calcination at 450°C as it is above the Tamman temperature for ~5nm Ag nanoparticles (220°C),{Luo, 2008 #70} where bulk diffusion becomes rapid.

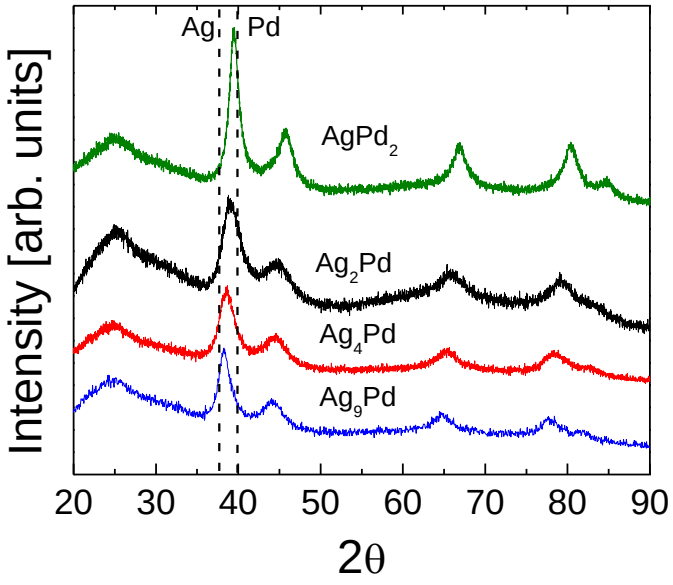

Figure S3: X-ray diffraction for all Pd:Ag ratios. The diffraction peaks shift linearly to higher two thetas as the amount of Pd increases in the alloy. The broad peaks from 20° to 30° correspond to the Vulcan XC72 carbon support. The particle sizes calculated from the (111) reflection with the Scherrer equation are summarized in Table 1.

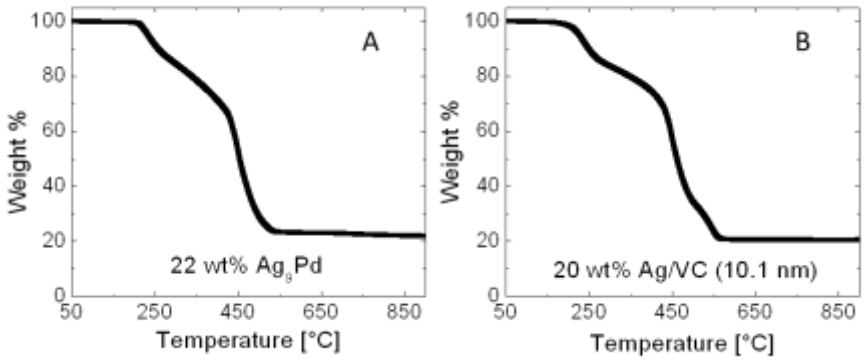

Figure S4: Thermogravimetric analysis for Vulcan XC72 carbon supported (A) Ag_9Pd and (B) Ag after calcination for activation and ligand removal. Each catalyst is loaded to ~20 wt% for an accurate comparison of activities.

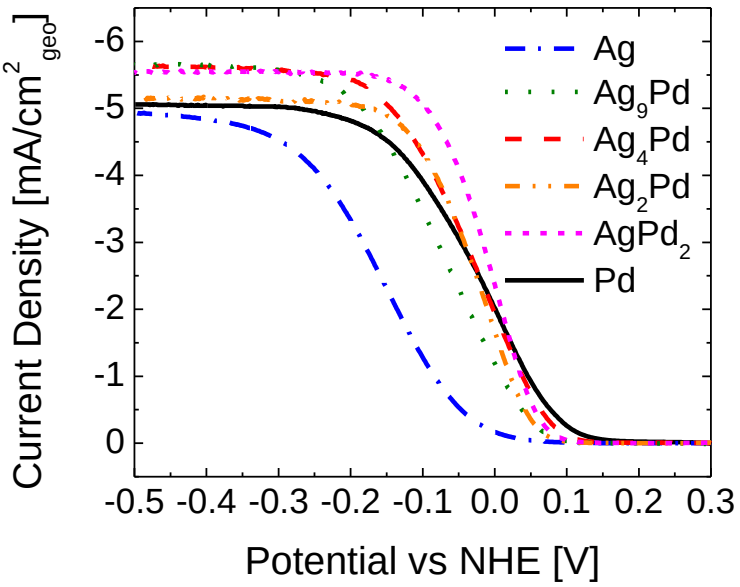

Figure S5: Polarization curves for all alloy ratios studied as well as pure Ag and commercial Pd.

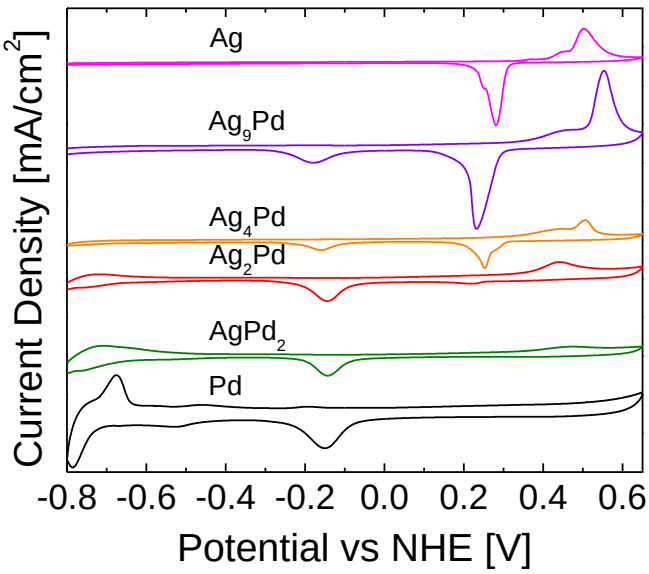

Figure S6: Cyclic voltammograms for all Ag:Pd ratios in Ar purged 0.1 M KOH. The surface characteristics change as the more Pd is added to the alloy. For dilute $Ag_{\geq 4}Pd$, the CVs resemble that of pure Ag, with the addition of a small Pd oxide reduction peak at ~-0.2V. For ratios of $Ag_{\leq 2}Pd$, the Ag oxidation peaks are diminished while the characteristic H_{upd} peaks (~-0.6V to -0.8V) for pure Pd emerge. As a minimum of Pd dimers in the surface is required for this H_{upd}, the alloy surface can be characterized Pd monomers dispersed in Ag for $Ag_{\geq 4}Pd$, whereas Pd clusters in Ag are present for $Ag_{\leq 2}Pd$.

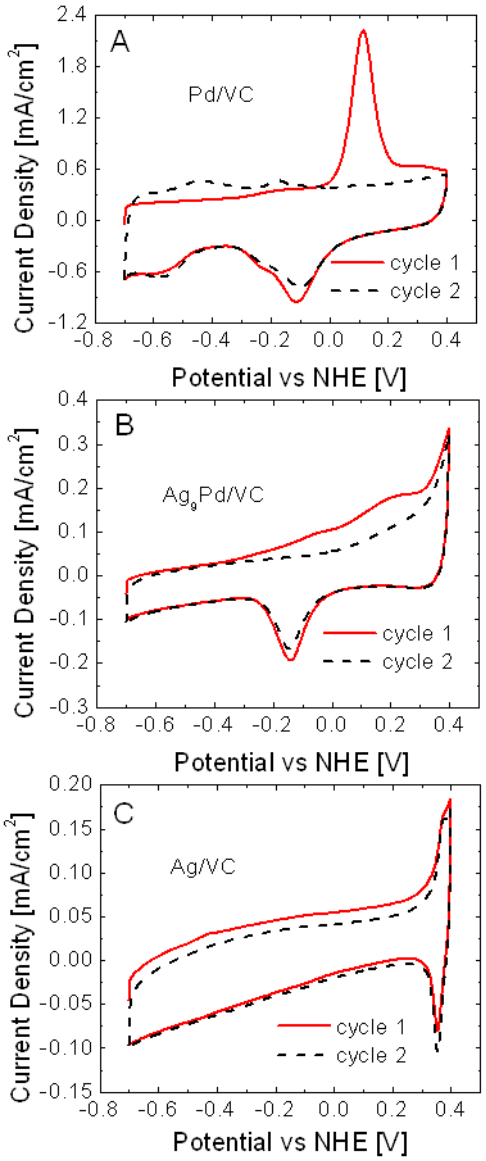

Figure S7: CO stripping voltammograms of Vulcan XC72 carbon supported (A) Pd, (B) Ag_9Pd, and (C) Ag. The stripping peak at ~0.12 V for pure Pd is not present for the pure Ag catalyst. The alloy catalyst displays a broad CO stripping curve from ~-0.1 V to 0.3V, indicating that the signal is not a combination of the pure components, but modified to a unique signature for the dilute Pd in Ag alloy surface.

Table S1. XPS shifts for the various alloy ratios.

Catalyst	**Pd $3d_{5/2}$ Peak [eV]**	**$\Delta Pd_{5/2}$ [eV]**	**Ag $3d_{5/2}$ Peak [eV]**	**$\Delta Ag_{5/2}$ [eV]**
Ag	--	--	368.25	0
Pd	335.55	0	**--**	**--**
Ag_9Pd	335.2	0.35	368.15	0.1
Ag_4Pd	335.16	0.39	368.01	0.24
Ag_2Pd	334.86	0.69	367.76	0.49
$AgPd_2$	335.46	0.09	367.61	0.64